Carbohydrate Polymers 87 (2012) 1159–1168

Contents lists available at SciVerse ScienceDirect

Carbohydrate Polymers

journal homepage: www.elsevier.com/locate/carbpol

Immune cell-specific delivery of beta-glucan-coated iron oxide nanoparticles for diagnosing liver metastasis by MR imaging

Hieu Vu-Quang[a,b], Muthunarayanan Muthiah[a,b], Hwa Jeong Lee[a,b], You-Kyoung Kim[c], Joon Haeng Rhee[b], Jae-Hyuk Lee[d], Chong-Su Cho[c], Yun-Jaie Choi[c], Yong Yeon Jeong[e], In-Kyu Park[a,b,*]

[a] Department of Biomedical Science, Research Institute of Medical Sciences, Chonnam National University Medical School, Gwangju 501-746, South Korea
[b] Clinical Vaccine R&D Center, Chonnam National University Hwasun Hospital, Jeonnam 519-763, South Korea
[c] Department of Agricultural Biotechnology and Research Institute for Agriculture and Life Sciences, Seoul National University, Seoul 151-921, South Korea
[d] Department of Pathology, Chonnam National University Hwasun Hospital, Jeonnam 519-763, South Korea
[e] Department of Radiology, Chonnam National University Hwasun Hospital, Jeonnam 519-763, South Korea

ARTICLE INFO

Article history:
Received 26 July 2011
Received in revised form 18 August 2011
Accepted 27 August 2011
Available online 12 September 2011

Keywords:
β-Glucan
Immune cells
Specific targeting
MR imaging
Liver metastasis

ABSTRACT

Glucans are reported to elicit immune responses through activation of macrophages by a specific interaction of β-glucan with an immune cell-specific (1,3)-β-D-glucan receptor or Dectin-1 receptor. In this study, superparamagnetic iron oxide nanoparticles (SPIONs) were coated with β-glucan in order to target the immune cells residing in the metastatic liver as an aid for discriminating metastasized tumor regions from normal hepatic parenchymal tissue. The morphology of prepared β-glucan-coated SPIONs (Glu-SPIONs) was characterized with dynamic light scattering (DLS) and transmission electron microscopy (TEM). The cytotoxicity of Glu-SPIONs was analyzed and compared to that of dextran- and PVA-coated SPIONs. The uptake of Glu-SPIONs by peritoneal macrophages was also confirmed with Prussian blue staining and MRI phantom tube imaging. The *in vivo* uptake of Glu-SPIONs in liver and lymph nodes in a metastatic mouse liver model was tracked by MR imaging after the systemic injection. The Glu-SPIONs predominantly accumulated in the macrophages surrounding the metastatic regions of the liver thereby indicating the distribution of tumor cells in the liver. MR imaging of the Glu-SPIONs clearly revealed macro- or micro-metastasized tumor regions throughout the liver, due to the preferential uptake of Glu-SPIONs into macrophages, not tumor cells. The Glu-SPION-accumulating regions were further confirmed with H&E and Prussian blue stainings after tissue sectioning. Based on our study, we propose that Glu-SPIONs can be successfully applied for diagnosing hepatic metastasis.

1. Introduction

The diagnosis of liver metastasis, which frequently occurs in patients with colon, lung, breast, and gastric cancer, is very important for cancer treatment. Many techniques have been used to diagnose liver metastases, including magnetic resonance imaging (MRI) (Bellin et al., 1994; Bipat et al., 2005; Namasivayam, Martin, & Saini, 2007; Rappeport & Loft, 2007), computed tomography (Okano et al., 2002), positron emission tomography (Nakamoto et al., 1999), and ultra-sound of the liver (Rummeny & Marchal, 1997). MRI is a non-invasive detection technique that provides excellent anatomical detail and soft tissue contrast, by detecting the level of proton contents within tissues. The specificity of the tissue of interest is commonly enhanced during imaging by the use of MRI contrast agents. Superparamagnetic iron oxide nanoparticles (SPIONs), which give a negative enhancement effect during the T2 sequence, is a frequently used MRI contrast agent that helps in detecting tumors as small as three millimeters in MR images (Namasivayam et al., 2007).

SPIONs have a high specific surface area, which provides an extensive contact between the surface and the aqueous dispersion medium. In the absence of an efficient surface coating, SPIONs can form agglomerates and aggregates due to the attractive forces between the hydrophobic magnetic nanoparticles, thereby destabilizing the suspension of nanoparticles in the medium. After intravenous administration, the hydrophobic surfaces of the aggregates become preferentially covered with plasma protein components, leading to opsonization, followed by rapid removal from the circulation by the reticulum endothelial system (RES). The aggregation of nanoparticles can be prevented by modifying the iron oxide surface using

* Corresponding author at: Department of Biomedical Science, Research Institute of Medical Sciences, Chonnam National University Medical School, Gwangju 501-746, South Korea. Tel.: +82 61 379 8481; fax: +82 61 379 8455.
E-mail address: pik96@chonnam.ac.kr (I.-K. Park).

0144-8617/$ – see front matter © 2011 Elsevier Ltd. All rights reserved.
doi:10.1016/j.carbpol.2011.08.091

A

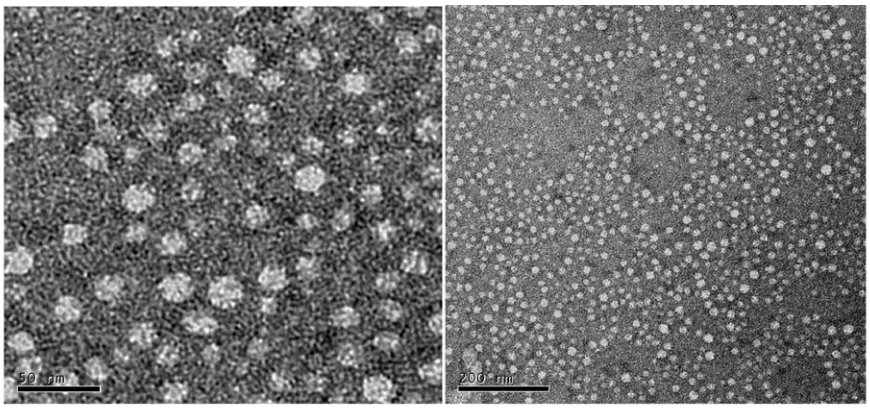

B

Scale bar: 50 nm Scale bar: 200 nm

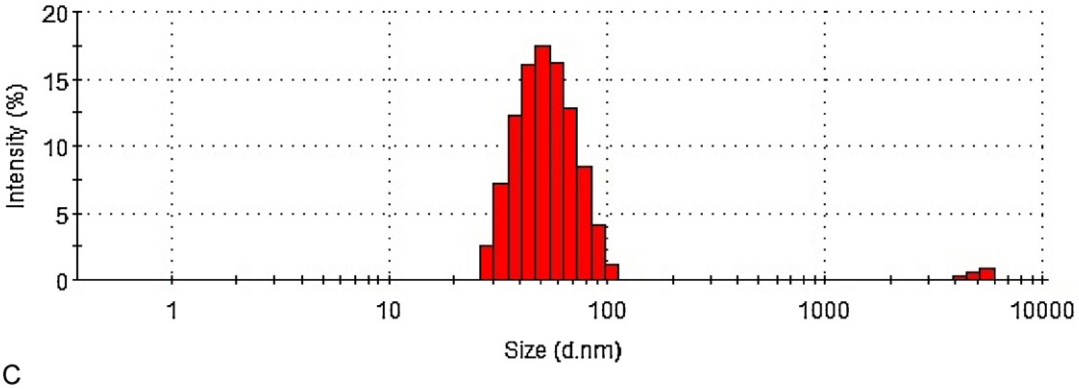

C

	SPION	β-glucan SPION
DLS	15.7 nm ± 6.3	51.8 nm ± 2.63
ζ- potetial	+4.44 mV ± 2.3	-11.42 mV ± 3.8

Fig. 1. (a) The morphology of Glu-SPIONs at varied magnifications measured by TEM. (b) The hydrodynamic particle size distribution of Glu-SPIONs measured by DLS. (c) Average particle size (nm) and surface charge (mV) of Glu-SPIONs.

biocompatible ligands and/or polymers which are attached at the particle surface by physical or chemical adsorption (Di Marco et al., 2007). These modifications can also improve hydrophilicity as well as direct the nanoparticles to specific cells.

β-Glucans are a heterogeneous group of glucose polymers, consisting of a backbone of β(1→3)-linked β-D-glucopyranosyl units bearing β(1→6) linked side chains with varying distributions and lengths (Cleary, Kelly, & Husband, 1999). The high biological activities of β-glucans are mainly attributable to their longer interaction with receptor-positive immune cells in mammalian systems (Nono, Ohno, Masuda, Oikawa, & Yadomae, 1991). Mammalian cells do not possess (1→3) β-glucanases and cannot rapidly degrade these carbohydrates; metabolism occurs slowly through oxidation. β-Glucans are taken up primarily by Kupffer cells in the liver, where they are slowly degraded (Suda et al., 1996). β-Glucan receptor activity has been reported in a variety of leukocytes, including macrophages, neutrophils, eosinophils, and NK cells. Non-opsonic recognition of β-glucan by these cells has been ascribed to multiple receptors, and a number of β-glucan receptors have been identified, including CR3, lactosyl ceramide, scavenger receptors, and Dectin-1.

Of these receptors, only Dectin-1 has been clearly shown to have a role in mediating the biological response to β-glucans. Dectin-1 recognizes carbohydrates containing β-1,3 and/or β-1,6 glucan linkages, and is expressed in immune cells like monocytes/macrophages, neutrophil lineages, dendritic cells and a subpopulation of splenic T cells (Brown & Gordon, 2003). Biological activities associated with *in vivo* use of these molecules include tumor inhibition, enhanced defense against bacterial challenge, increased hemopoeitic activity, radio-protective effects, and improved wound healing. An *in vitro* study with β-glucan reported that these molecules influenced macrophage morphology, release of cytokines (such as TNF-a, IL-6 and IL-1), release of nitric oxide, hydrogen peroxide release, and alternate pathway complement activation (Suzuki, Ohno, Saito, & Yadomae, 1992). The major mechanism by which glucans are thought to elicit these responses is through activation of macrophages, possibly via a macrophage

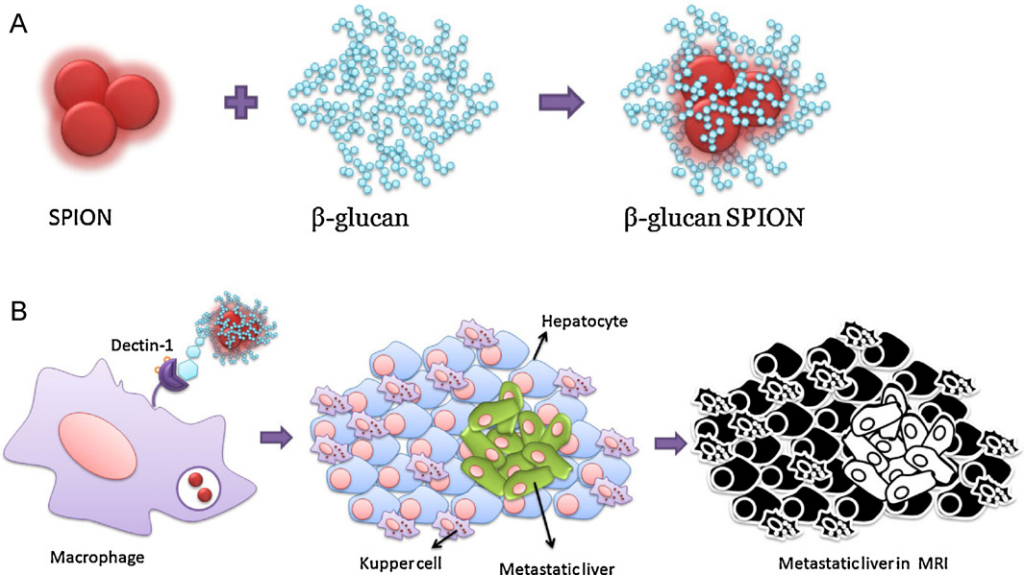

Scheme 1. (A) Glu-SPION preparation scheme. (B) Mechanism for the diagnosis of metastatic liver by MR imaging. Glu-SPION was recognized by the Dectin-1 receptor expressed on the APC surface and was then phagocytosed. After I.V. administration, Glu-SPION was specifically phagocytosed by Kupffer cells located in the liver. When imaged through MRI, a tumor region will appear brighter than regions of the liver that are rich in macrophage cells that have accumulated Glu-SPIONs. Thus, a metastasized region in the liver can be readily distinguished from the normal regions.

specific (1,3)-β-D-glucan receptor, or through binding to the complement receptor CR3 (CD11b/CD18). Another recent report also demonstrated that glucan could directly influence the activity of other immune cells, including T and B cells, NK cells, eosinophils, and neutrophils (Cleary et al., 1999).

In the present study, β-glucan-coated SPIONs (Glu-SPIONs) were prepared and their specific uptake by immune cells such as peritoneal macrophages and dendritic cells was analyzed. The cytotoxicity of Glu-SPIONs was compared to that of dextran- and PVA-coated SPIONs (Dex-SPIONs and PVA-SPIONs, respectively). The *in vitro* uptake of Glu-SPIONs by peritoneal macrophages was confirmed with Prussian blue staining and MRI phantom tube imaging. The *in vivo* accumulation of the particles in liver and lymph node was also tracked with MRI in a metastatic mouse liver model.

2. Materials and methods

2.1. Synthesis of Glu-SPIONs

The Glu-SPIONs were synthesized, with some modifications, according to a previous publication (Yoo et al., 2008). SPIONs were prepared by alkaline co-precipitation of $FeCl_3{\cdot}6H_2O$ and $FeCl_2{\cdot}4H_2O$ (Sigma–Aldrich, MO, USA) with a Fe(III)/Fe(II) feed ratio of 3:1 in the deoxygenated water following the addition of NH_4OH. The black precipitate was washed multiple times and the final pH was adjusted down from 10 to 7. The solution was allowed to sediment under a magnetic field and the supernatant was discarded. The black sediment was mixed with 2 M HNO_3 and 0.35 M $Fe(NO_3)_3$. The suspension was dialyzed for 2 days against 0.01 M HNO_3, and stored at 4 °C. Finally, the product was co-incubated with β-glucan (Wako, Osaka Japan) in order to obtain Glu-SPIONs, and the pH was adjusted to 7 by using NH_4OH. The other contrast agents, Dex-SPIONs and PVA-SPIONs, were also prepared by the same method.

2.2. Size and morphology of Glu-SPIONs

The sizes of SPIONs were assessed at 25 °C using an electrophoretic light scattering spectrophotometer (ELS 8000, Otsuka Electronics, Osaka, Japan) with 90° and 20° scattering angles. Electrophoretic mobility was measured using the same setup equipped with a platinum electrode. The morphology of Glu-SPIONs was assessed using a FEI Tecnai F20 transmission electron microscope (TEM). For TEM sample preparation, the Glu-SPIONs were diluted in distilled water, and a droplet was placed on a copper grid mesh and allowed to dry. Excess droplet material was removed from the grid, and the particles were observed directly by TEM, with no further staining.

2.3. Primary peritoneal macrophage isolation

Three days after intraperitoneal injection of 3 mL Brewer thioglycolate medium into inbred Balb/c 7 weeks old male mice (Orient Bio Inc., Seongnam-si, South Korea), peritoneal macrophages were

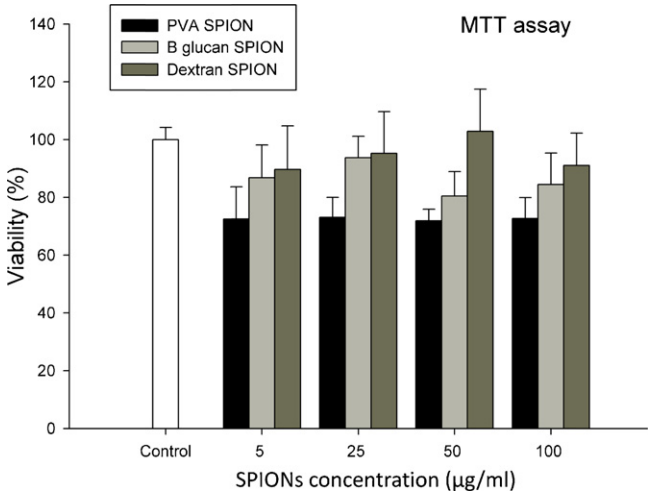

Fig. 2. Cytotoxicity assay. Murine peritoneal macrophages were seeded on 96 well plates (2×10^4 cells/well). Glu-SPIONs, PVA-SPIONs, and Dex-SPIONs were added at various concentrations (5, 25, 50, and 100 μg Fe/mL) and incubated for 24 h. MTT assays were performed following a standard protocol ($n = 4$).

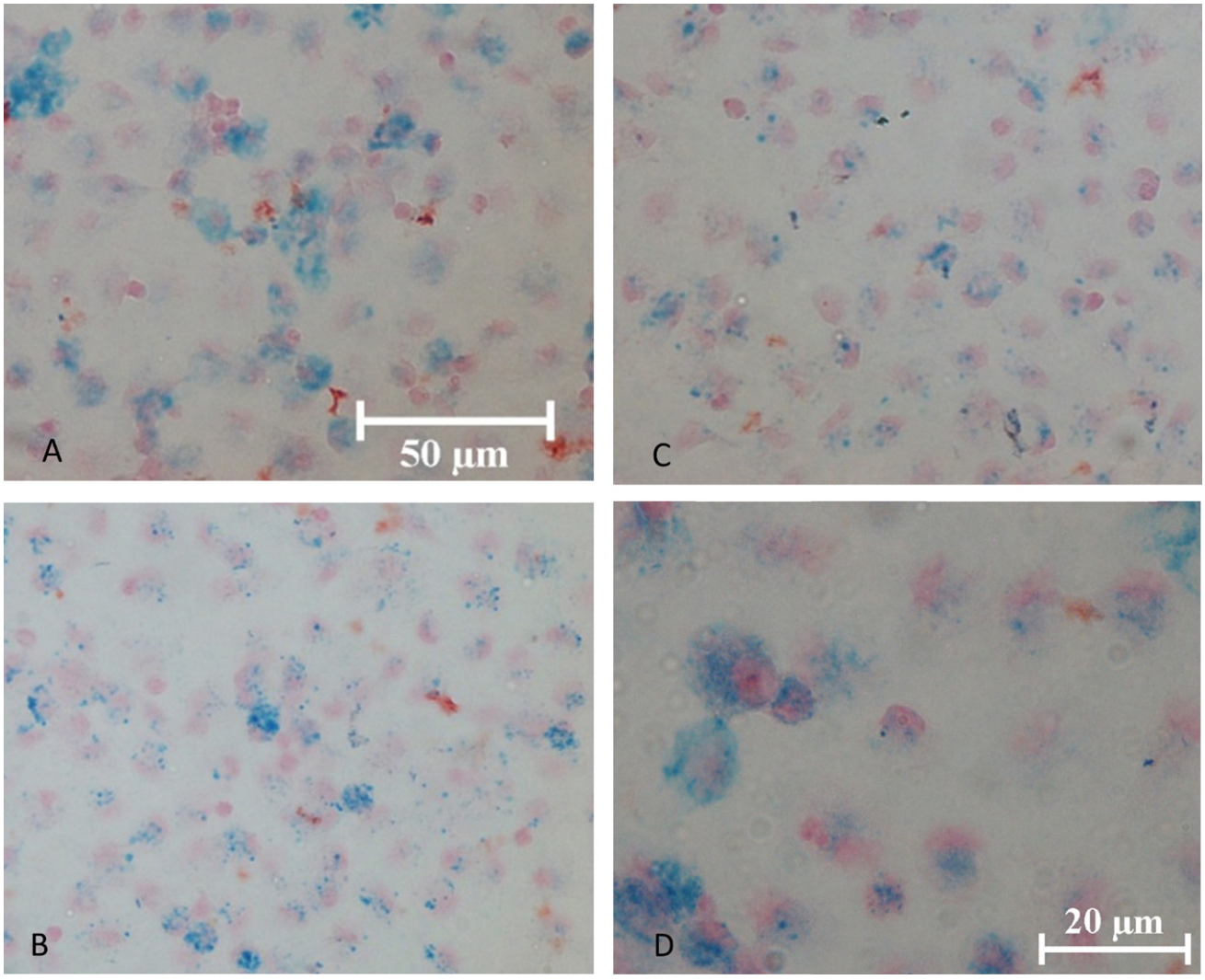

Fig. 3. *In vitro* intracellular uptake of Glu-SPIONs in murine-derived primary peritoneal macrophages. Fresh peritoneal macrophages were isolated and incubated with Glu-SPIONs, PVA-SPIONs, and Dex-SPIONs (100 μg Fe/mL) on cell culture treated glass slides for 3 h. Each slide was then stained with Prussian blue reagent. Glu-SPION (a), PVA-SPION (b), Dextran-SPION (c), Glu-SPION at higher magnification (d). Blue: iron, pink: nucleus. (For interpretation of the references to color in this figure legend, the reader is referred to the web version of the article.)

collected by injecting 7 mL of serum free ice cold RPMI 1640 (Thermo Scientific, UT, USA) twice into the peritoneal cavity. The fluid was collected, centrifuged, treated with ACK buffer (Lonza Walkersville, MD, USA) for 5 min, and washed with PBS 3 times at 1000 rpm for 10 min. Cells were allowed to adhere to the cell culture dish for 2 h in serum free RPMI 1640 in a 5% CO_2 atmosphere at 37 °C. The dish was then washed 3 times with cold PBS to remove non-adherent cells. Adherent cells were harvested with a cell scraper.

2.4. Cytotoxicity of Glu-SPIONs

Isolated peritoneal macrophages were seeded in 96 well plates at density 2×10^4/well in 100 μL of RPMI 1640 growth medium and incubated overnight at 37 °C in 5% CO_2. The cells were treated with Glu-SPIONs, Dex-SPIONs, and PVA-SPIONs at various concentrations (5, 25, 50, and 100 μg Fe/mL) for 24 h. The cells were incubated with 100 μL of MTT solution for 4 h to allow formation of formazan crystals by mitochondrial dehydrogenases. The medium was removed and 100 μL of DMSO was added to dissolve the formazan crystals. The optical density of the solution was measured at a wavelength of 570 nm using a Spectra Max 190 spectrophotometer (Molecular Devices, Sunnyvale, CA, USA).

2.5. In vitro uptake of Glu-SPIONs by peritoneal macrophages

Macrophages were harvested and cultured with a cell density of 5×10^5 cells/well in a 24-well plate in 500 μL of RPMI 1640 growth medium. The macrophages were incubated with the determined amount of Glu-SPIONs (iron conc. 100 μg Fe in each well). At 1, 2, 3, and 24 h post-incubation, the treated macrophages were harvested, washed three times with PBS, and then fixed with 4% HCHO. The fixed macrophage cells were stained with Prussian blue. The intracellular accumulation of Glu-SPIONs by mouse peritoneal macrophages was evaluated semi-quantitatively by MRI. The fixed cells were counted again and embedded in gelatin 10% (1:1). Next, the middle gelatin layer was placed in 0.5 mL Eppendorf tubes for *in vitro* phantom MRI measurements. The MR phantom tubes were placed in a water bath inside the magnetic field (b0) of a MRI machine. MRI scanning was performed with a 3.0 T clinical whole-body MR unit (Siemens Magneto Tim Trio 3.0 T, wrist coil). The MR sequence was a two-dimensional (2D) gradient-echo sequence with TR = 3000, TE = 75,

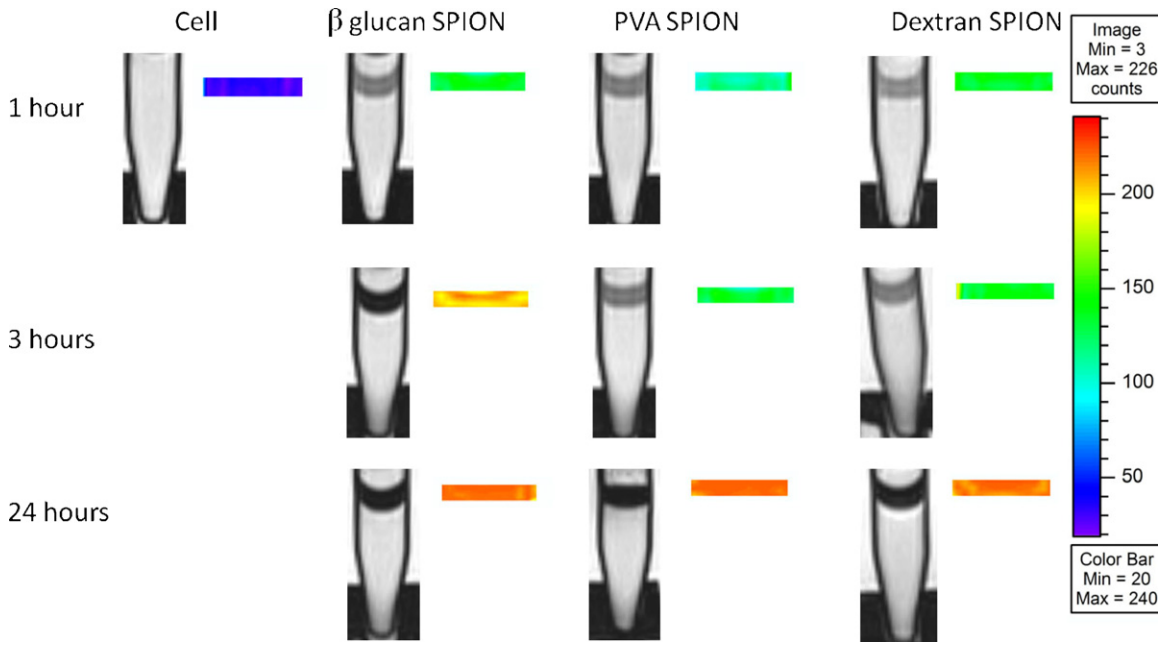

Fig. 4. MR phantom tube imaging of peritoneal macrophages following accumulation of Glu-SPIONs, PVA-SPIONs, and Dex-SPION at various time points (1, 3 and 24 h). The pseudo-color image was converted by Living Image software. (For interpretation of the references to color in this figure legend, the reader is referred to the web version of the article.)

NEX = 4, slice thickness = 2 mm, flip angle = 150 and field of view (FOV) = 214 × 384.

2.6. Prussian blue staining

Paraffin blocks were prepared from the fixed peritoneal macrophages and tissue samples and processed for Prussian blue staining. Each paraffin-embedded sample was sliced into 5 μm sections, which were placed on glass slides. The sections were deparaffinized and serially hydrated by immersing the slides twice in 100% xylene, twice in 100% ethanol, and once in 95%, 90%, 80%, and 70% ethanol. The hydrated slides were washed under tap water for 5 min and stained with 1:1 mixture of 20% HCl and 10% potassium ferrocyanide trihydrate for 20 min. The slides were then counterstained with Nuclear Fast Red solution (Sigma–Aldrich, MO, USA) for 5 min. The stained slide was mounted in Permount solution (Fisher Scientific, PA, USA).

2.7. Mouse liver metastatic model

A CT-26 colorectal carcinoma cell line was cultured at 37 °C in 5% CO_2 in DMEM growth medium (WELGENE Inc., Korea), supplemented with 10% FBS, 100 μg/mL streptomycin, and 100 units/mL penicillin. The establishment of metastatic liver was described previously (Jain et al., 2003). In short, BALB/c mice were anesthetized by administration of 3 mL avertin. The hair was removed from the mouse's left flank and a small incision was made to expose the spleen. The spleen was tied by sutures and cut into 2 pieces. With a 29-gauge needle, 2×10^5 CT-26 cells in 200 μL of PBS were injected to one piece of the hemi spleen. The CT-26 cells migrate to the liver via the vein. After 5 min, the splenic vein was tied by sutures and the injected spleen was cut. Metastatic livers were allowed to develop for two weeks.

2.8. MRI determination of in vivo distribution

The accumulation of the SPIONs in liver of the Balb/c mouse (7 weeks, male) (Orient Bio, Korea) was confirmed by MRI. Mice were

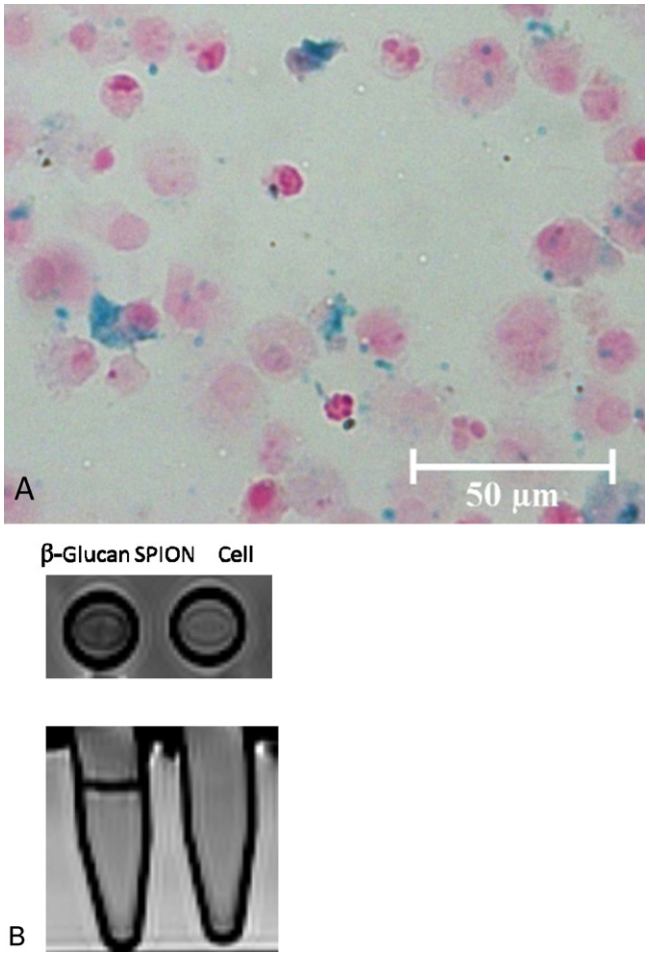

Fig. 5. *In vitro* uptake of Glu-SPIONs in murine bone marrow derived DCs. Glu-SPIONs were incubated for 3 h with monocytes derived from murine bone marrow dendritic cell. Prussian blue stained DC (a), MR phantom tube imaging of Glu-SPION-treated DC (b), the untreated dendritic cells were taken as control.

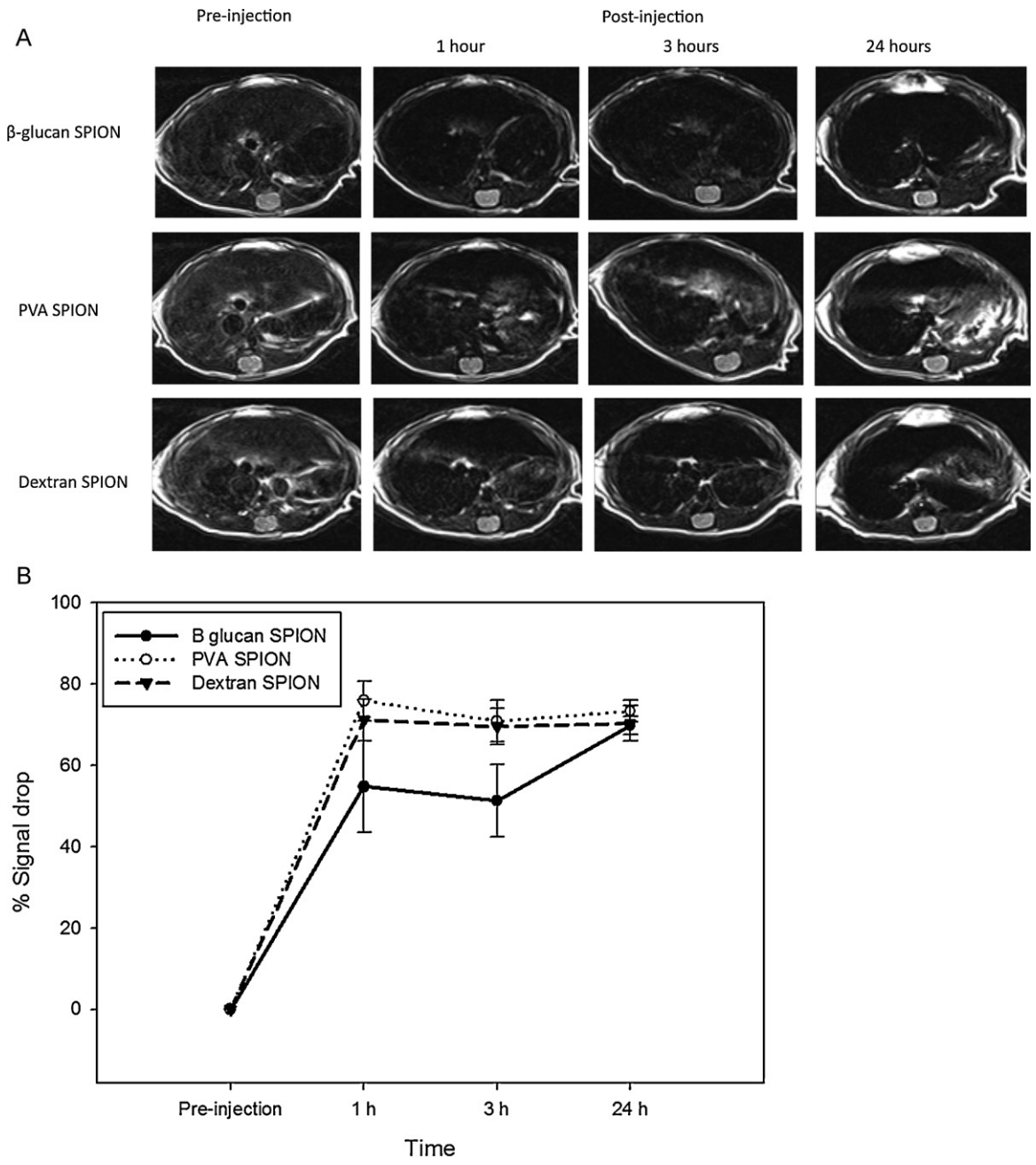

Fig. 6. MR imaging of Glu-SPIONs, PVA-SPIONs, and Dex-SPIONs accumulated in the normal liver. (a) MR imaging of mouse liver regions after systemic administration of 500 μL of Glu-SPIONs, PVA-SPIONs, and Dex-SPIONs (5 μg Fe/μL). (b) The time-dependent drop in MR T2 signal intensities measured in the liver after the administration of Glu-SPIONs, PVA-SPIONs, and Dex-SPIONs ($n = 5$). Histology of the accumulated Glu-SPIONs in mouse liver after systemic injection. (c) H&E staining, (d) Prussian blue staining. After MR measurements, the liver was isolated and stained with Prussian blue. Arrows indicate iron accumulation; blue: iron, red: nucleus. Magnification: 40×, scale bar: 500 μm. (For interpretation of the references to color in this figure legend, the reader is referred to the web version of the article.)

anesthetized with Isoflurane 2% (Choongwae, Seoul, Korea) and pre-scanned using clinical MRI equipment (Siemens mouse coil) on the liver area. All experiments were performed after approval by our local ethical committee at Chonnam National University Medical School and in accordance with principles of laboratory animal care (CNU IACUC-H-2011-5). The scanning procedure included the acquisition of T2 weighted spin echo coronal anatomical images for localization of liver (measured parameters: slice thickness 1 mm, matrix 256 × 218, TR = 3000 ms, NEX = 2, TE = 104 ms, 1 average (FOV) 100 mm × 100 mm and flip angle = 150). After the first scan, mice were intravenously injected into the tail vein with Glu-SPIONs, Dex-SPIONs, and PVA-SPIONs at doses of 12.5 mg Fe/kg (3 mice in each group) and scanned on the same locations at 1, 3 and 24 h post-injection. Mice were sacrificed after the last scan. The liver and inguinal lymph node were removed and fixed in 4% HCHO for Prussian blue staining. Signal intensities from the muscle region and liver were measured and converted to the relative intensity ratio between lymph node and muscle. The signal intensity ratio from the pre-scanning imaging was set at 100%.

3. Results and discussion

Conjugation of SPIONs with target molecules or loading them into target cells, can provide the targeted molecule or cells with

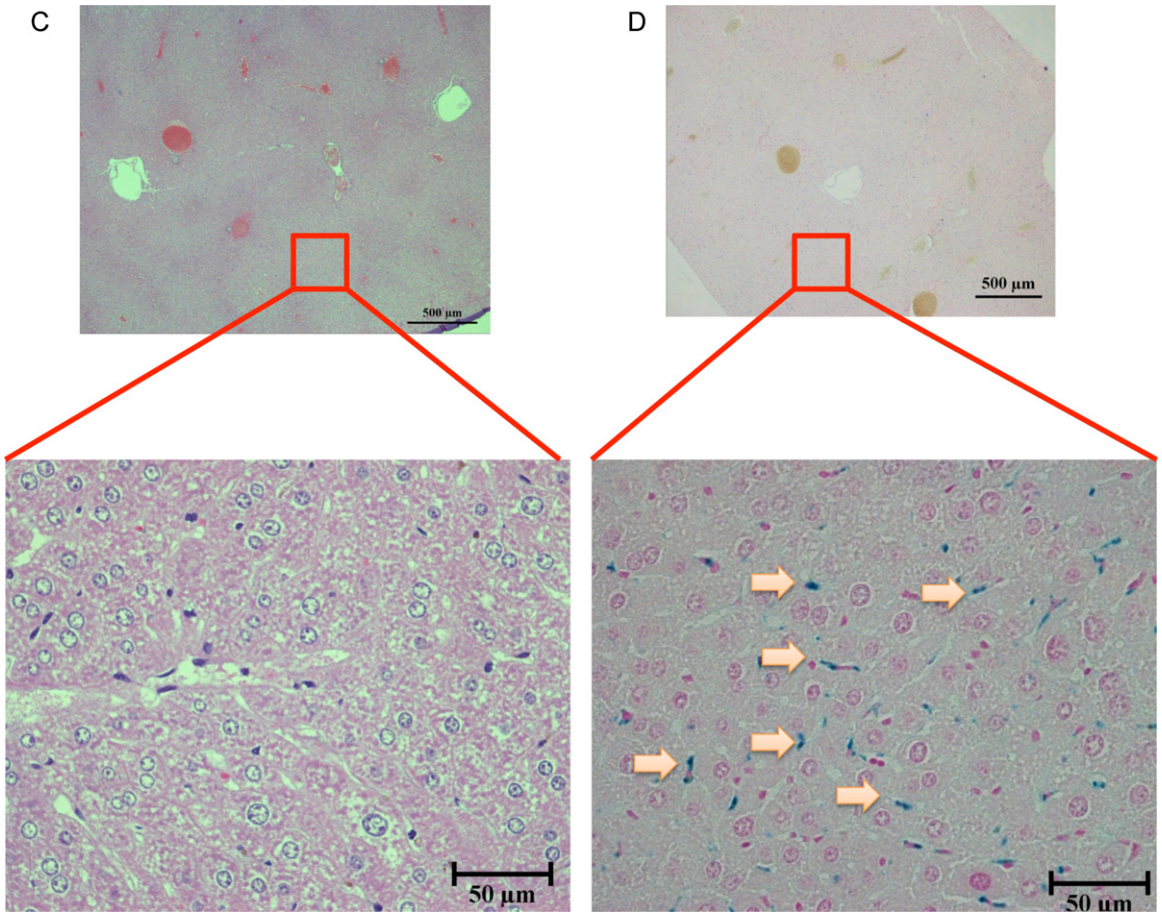

Fig. 6. (*Continued*)

a large magnetic moment that creates substantial disturbances in the local magnetic field, which leads to a rapid dephasing of protons. This property of SPIONs allows tracking of target molecules or loaded cells by non-invasive MR imaging. The Glu-SPIONs were targeted to the immune cells in the liver. The injected Glu-SPIONs were taken up by the Kupffer cells, which are specialized macrophages in the liver. Abnormal proliferation of tumor tissues causes a local lack of Kupffer cells, which resulted in an unaltered MR signal intensity because of poor accumulation of SPIONs. These Kupffer cells-deficient tumor regions can be discriminated from the surrounding SPION-rich normal tissues (Bulte, 2004).

The Glu-SPION accumulation in Kupffer cells also induces their activation, as well as the stimulation of the other immune cells, resulting in the release of inflammatory mediators. The Glu-SPIONs also activate neutrophils and natural killer cells to a tumoricidal state (Sveinbjornsson, Rushfeldt, Seljelid, & Smedsrod, 1998). The aim of the present study was to fabricate Glu-SPIONs that would specifically target the immune cells and to study the localization of immune cells-rich organs such as liver and lymph node after systemic injection of Glu-SPIONs. The specific accumulation of Glu-SPIONs in the immune cells of the hepatic system was examined by its potential diagnostic value for identifying liver metastatic regions (Scheme 1).

In this work, the SPIONs were coated with β-glucan in order to target specific receptors like Dectin-1 in the immune cells. The specific interactions of the Glu-SPIONs with peritoneal macrophages and dendritic cells were studied *in vitro*. The Glu-SPIONs were systemically injected, and their accumulation in the liver and lymph nodes was confirmed with *in vivo* MR imaging and histochemical analysis.

3.1. Characteristics of Glu-SPIONs

SPIONs were coated with β-glucan to improve aqueous stability, to prevent aggregation, and to target them to immune cells including antigen-presenting cells (APCs). The parent SPION nanoparticles, synthesized by co-precipitation of ferrous and ferric ions, were prepared for the specificity to immune cells by adsorption of β-glucan on the surface of magnetic nanoparticles. Hydrogen bonding is assumed to be the predominant mechanism for the adsorption of a non-ionic polymer such as β-glucan onto the oxide surface of magnetic nanoparticles, which occurs through the interaction between polar functional groups of β-glucan and hydroxylated and/or protonated ones of the iron oxide nanoparticles (Petri-Fink, Chastellain, Juillerat-Jeanneret, Ferrari, & Hofmann, 2005).

The application of a β-glucan coating onto SPIONs increased their dispersal in water. The size and morphology of the Glu-SPIONs was analyzed by DLS and TEM, respectively. The particle sizes of SPION before and after coating with β-glucan were around 15.7 ± 6.3 nm and 51.8 ± 2.63 nm, respectively. Zeta potential measurement revealed surface charges of the uncoated SPIONs and Glu-SPIONs of approximately +4.44 mV and −11.42 mV, respectively (Fig. 1). The TEM images of Glu-SPIONs showed uniform and spherical morphologies of about 20 nm in diameter in aqueous solution. The presence of the negative surface charge on the

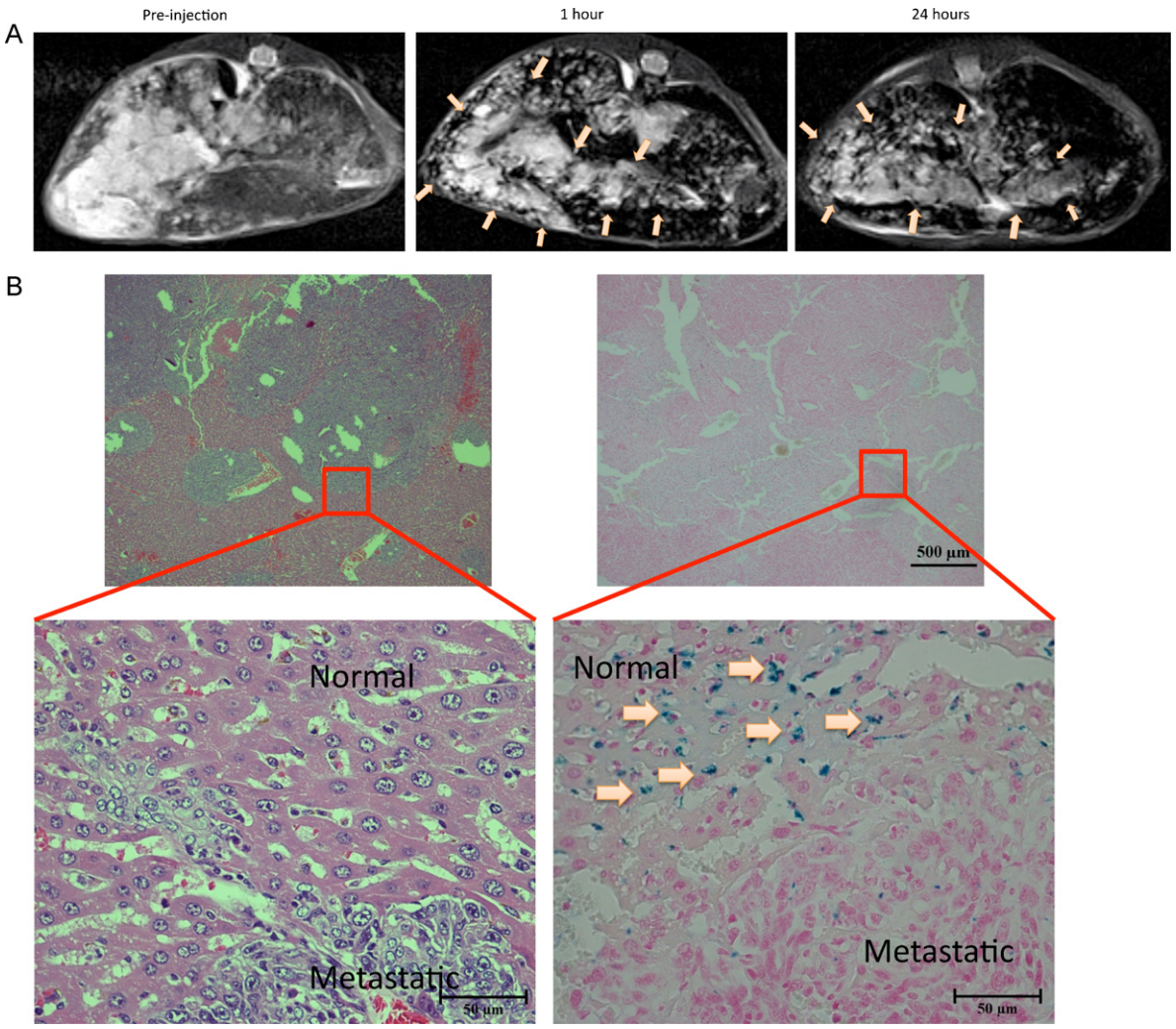

Fig. 7. MR imaging and a pathologic specimen for a partially metastatic liver. (a) Time course MR images of metastatic liver after systemic injection of Glu-SPIONs. The CT-26 colon cancer cells (10^7 cells) were subcutaneously injected into a Balb/c mouse. Three weeks after the inoculation, the mouse was intravenously injected with Glu-SPIONs. The liver was scanned by MRI both at the pre- and post-injection sites. The liver was isolated for Prussian blue and H&E staining. Arrows indicate the bright areas in liver, representing the hepatic metastatic region. (b) Histological analysis of Prussian blue stained liver demonstrated the accumulation of Glu-SPIONs into immune cell-rich regions in normal liver. H&E staining (left panel) and Prussian blue staining (right panel). Proliferating tumor cells stained by H&E staining are distinguishable.

particles has been reported to induce an intracellular uptake three orders of magnitude higher than that of conventional dextran-coated SPIONs (Bulte & Kraitchman, 2004).

3.2. Cytotoxicity of Glu-SPIONs

Cell viability was evaluated following addition of Glu-SPIONs, PVA-SPIONs, and Dex-SPIONs at various concentrations. Fig. 2 shows the MTT assay results for cytotoxicity of these SPIONs against murine peritoneal macrophage cells isolated from the peritoneal cavity. When the iron concentration was increased, the cell viability of Glu-SPION-treated group was minimally affected, indicating that Glu-SPIONs have a similar cytotoxicity level to that of Dex-SPIONs, a contrast agent currently used in clinical diagnosis (Clement, Siauve, Cuenod, & Frija, 1998; Corot, Robert, Idee, & Port, 2006; Misselwitz, 2006), and a lower cytotoxicity than PVA SPIONs. Therefore, Glu-SPIONs appear to be useful as a non-toxic contrast agent for MRI.

3.3. In vitro uptake of Glu-SPIONs

Intracellular residence of the particles was validated by Prussian blue staining. The blue dots indicate the presence of iron inside the macrophage and the pink represents the nucleus. The cells were treated with Glu-SPIONs, PVA-SPIONs, and Dex-SPIONs (Fig. 3) and stained with Prussian blue 3 h after the treatment to analyze the intracellular uptake of the SPION particles by the respective cells. The particles were clearly recognized and phagocytosed by peritoneal macrophages. The intracellular accumulation of Glu-SPION in macrophages was higher than of the accumulation of either PVA-SPIONs or Dex-SPIONs. The intracellular localization of Glu-SPIONs was observed in the cytoplasm of these cells, which is visible from Fig. 3d.

The macrophage cells were treated with Glu-SPIONs, PVA-SPIONs, and Dex-SPIONs and placed between two gelatin layers. The MR signal drop from the phantom tubes containing the macrophage cells treated with respective SPION particles was analyzed according to time course post-incubation, as shown in Fig. 4. At 1 h post-incubation, the drop in the MR signal intensity was almost the same for all three samples. However, after 3 h, a significant drop in MR signal intensity was noted for the phantom tube containing the macrophages incubated with Glu-SPIONs. This indicated preferential uptake of Glu-SPIONs by macrophages compared to uptake of PVA-SPIONs and Dex-SPIONs, which was possibly as a result of specific interaction between the β-glucan on the Glu-SPIONs and specific receptors such as Dectin-1 on the macrophage cells. Receptor-targeted uptake by macrophages was rapid, which

was also demonstrated in our previous publication where the mannose receptor on macrophages was successfully targeted with mannan-coated SPIONs. A greatly facilitated uptake of mannan-coated SPIONs into macrophages was found when compared to uptake of Dex-SPIONs and PVA-SPIONs (Vu-Quang et al., in press).

Murine bone marrow derived dendritic cells (DCs) were treated with Glu-SPIONs and stained after 3 h of incubation, to confirm the cellular uptake of Glu-SPIONs. The particles were phagocytosed by DCs and the accumulation was observed in the cytoplasm (Fig. 5a). This similarity of this result to that obtained with Glu-SPION-treated peritoneal macrophages confirmed the uptake of Glu-SPIONs in the APCs. The uptake of the Glu-SPIONs in DCs was also confirmed by MRI, which showed a significant MR signal drop on the phantom tube having a layer of DCs labeled with Glu-SPIONs compared to a DC control (Fig. 5b). In an *in vitro* study, Glu-SPIONs were expected to bind to the APCs mainly by the interaction with Dectin-1 and CR-3 receptors (Herre, Gordon, & Brown, 2004; McCann, Carmona, Puri, Pagano, & Limper, 2005; Ross, Vetvicka, Yan, Xia, & Vetvickova, 1999; Thornton, Vetvicka, Pitman, Goldman, & Ross, 1996), which may then activate other immune system factors against tumors.

3.4. *In vivo* macrophage targeting

Glu-SPIONs, PVA-SPIONs, and Dex-SPIONs were systemically injected into mice and the change in MR signal drop was measured on the target organ before and after the treatment (Fig. 6a). The administered SPIONs accumulated in the normal liver, and no signal appeared in other organs, confirming the final destination of the samples. The Glu-SPION accumulation in the normal liver was comparable to that for PVA-SPIONs and Dex-SPIONs (Fig. 6b). The accumulation of Glu-SPIONs in the liver was confirmed by H&E and Prussian blue staining of the liver tissue sections after the systemic injection (Fig. 6c and d). Beta-glucan-SPION was uptaken by antigen presenting cells such as dendritic cells and macrophages. It was demonstrated that beta-glucan-SPION has preferential uptake in both primary cells in *in vitro*. However, it was thought that in *in vivo* study, the injected beta-glucan-SPION may have a frequent encounter with circulating immune cells like macrophages, DC and NK cells and then bound to them before reaching the target liver, which explains the delayed uptake in liver. DC and macrophage cells internalized with beta-glucan-SPIONs might migrate to lymph nodes efficiently. On the other hand, Dextran- and PVA-coated SPIONs have little specific interaction with circulating immune cells such as DC and NK cells. Thus, it was assumed that the faster uptake of Dextran- and PVA-coated SPIONs in liver might result from no specific interaction with immune cells whose receptors have specific binding to beta glucan.

Glu-SPIONs, PVA-SPIONs, and Dex-SPIONs were administered to the metastatic mouse liver model and imaged before and after injection (Fig. 7). At 1 h after the administration, the signal intensity in the liver started decreasing in the regions surrounding the metastatic region. After 24 h, a substantial intensity difference was evident between metastatic and normal regions and the tumor region could clearly be distinguished from the normal liver regions. The immunohistochemical analysis with H&E staining and Prussian blue staining confirmed Glu-SPION accumulation in the Kupffer cells, located in the normal immune cells-rich region in the liver, whereas no staining was found in the regions of highly metastatic and immune cell-deficient tumor regions in the liver (Fig. 7b). The administered Glu-SPIONs also had reached the immune cell-rich lymph nodes. The presence of Glu-SPIONs in the lymph node was confirmed by Prussian blue staining of the lymph node tissue (Fig. 8).

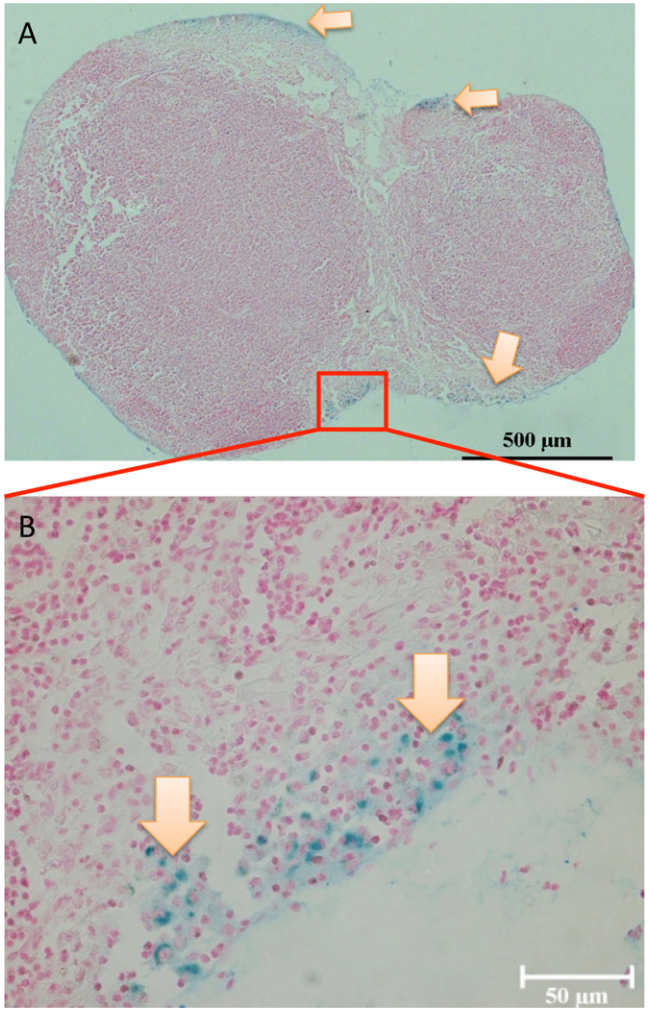

Fig. 8. Histology of the accumulated Glu-SPIONs in mouse lymph nodes after systemic injection in liver. After MR measurements, lymph nodes were also isolated and stained with Prussian blue. Arrows indicate the accumulation of iron; blue: iron, red: nucleus. Magnification: 40×, scale bar: 500 μm. (For interpretation of the references to color in this figure legend, the reader is referred to the web version of the article.)

4. Conclusion

In this study, Glu-SPION was prepared and targeted to immune cells in the liver for the detection of metastatic liver. The *in vitro* uptake of Glu-SPION has been confirmed with different immune cells by Prussian blue staining and MRI phantom tube imaging. The *in vivo* accumulation in the Kupffer cells, discriminating the metastatic tumor from the normal region, as well as in lymph nodal immune cells has been demonstrated successfully.

Acknowledgements

This work was financially supported by the Bio Imaging Research Center at GIST. IKP also acknowledges financial support from the Regional Technology Innovation Program of the Ministry of Commerce, Industry and Energy (Grant RT104-01-01); the Basic Science Research Program through the National Research Foundation of Korea, funded by the Ministry of Education, Science and Technology (2010-0002940); the Korea Healthcare Technology R&D Project, Ministry for Health, Welfare & Family Affairs, Republic of Korea (A084869 and A100553); and the Pioneer Research Center Program through the National Research Foundation of Korea

funded by the Ministry of Education, Science and Technology (M10711060001-08M1106-00110).

References

Bellin, M. F, Zaim, S., Auberton, E., Sarfati, G., Duron, J. J., Khayat, D., et al. (1994). Liver metastases: Safety and efficacy of detection with superparamagnetic iron oxide in MR imaging. *Radiology*, *193*(3), 657–663.

Bipat, S., van Leeuwen, M. S., Comans, E. F., Pijl, M. E., Bossuyt, P. M., Zwinderman, A. H., et al. (2005). Colorectal liver metastases: CT, MR imaging, and PET for diagnosis—meta-analysis. *Radiology*, *237*(1), 123–131.

Brown, G. D., & Gordon, S. (2003). Fungal beta-glucans and mammalian immunity. *Immunity*, *19*(3), 311–315.

Bulte, J. W. M. (2004). MR contrast agents for molecular and cellular imaging. *Current Pharmaceutical Biotechnology*, *5*(6), 483.

Bulte, J. W. M, & Kraitchman, D. L. (2004). Iron oxide MR contrast agents for molecular and cellular imaging. *NMR in Biomedicine*, *17*(7), 484–499.

Cleary, J. A, Kelly, G. E., & Husband, A. J. (1999). The effect of molecular weight and beta-1,6-linkages on priming of macrophage function in mice by (1,3)-beta-D-glucan. *Immunology and Cell Biology*, *77*(5), 395–403.

Clement, O., Siauve, N., Cuenod, C. A., & Frija, G. (1998). Liver imaging with ferumoxides (Feridex): Fundamentals, controversies, and practical aspects. *Topics in Magnetic Resonance Imaging*, *9*(3), 167–182.

Corot, C., Robert, P., Idee, J. M., & Port, M. (2006). Recent advances in iron oxide nanocrystal technology for medical imaging. *Advanced Drug Delivery Reviews*, *58*(14), 1471–1504.

Di Marco, M., Sadun, C., Port, M., Guilbert, I., Couvreur, P., & Dubernet, C. (2007). Physicochemical characterization of ultrasmall superparamagnetic iron oxide particles (USPIO) for biomedical application as MRI contrast agents. *International Journal of Nanomedicine*, *2*(4), 609–622.

Herre, J., Gordon, S., & Brown, G. D. (2004). Dectin-1 and its role in the recognition of beta-glucans by macrophages. *Molecular Immunology*, *40*(12), 869–876.

Jain, A., Slansky, J. E., Matey, L. C., Allen, H. E., Pardoll, D. M., & Schulick, R. D. (2003). Synergistic effect of a granulocyte-macrophage colony-stimulating factor-transduced tumor vaccine and systemic interleukin-2 in the treatment of murine colorectal cancer hepatic metastases. *Annals of Surgical Oncology*, *10*(7), 810–820.

McCann, F., Carmona, E., Puri, V., Pagano, R. E., & Limper, A. H. (2005). Macrophage internalization of fungal beta-glucans is not necessary for initiation of related inflammatory responses. *Infection and Immunity*, *73*(10), 6340–6349.

Misselwitz, B. (2006). MR contrast agents in lymph node imaging. *European Journal of Radiology*, *58*(3), 375–382.

Nakamoto, Y., Higashi, T., Sakahara, H., Tamaki, N., Kogire, M., Imamura, M., et al. (1999). Contribution of PET in the detection of liver metastases from pancreatic tumours. *Clinical Radiology*, *54*(4), 248–252.

Namasivayam, S., Martin, D. R., & Saini, S. (2007). Imaging of liver metastases: MRI. *Cancer Imaging*, *7*, 2–9.

Nono, I., Ohno, N., Masuda, A., Oikawa, S., & Yadomae, T. (1991). Oxidative degradation of an antitumor (1→3)-beta-D-glucan, grifolan. *Journal of Pharmacobio-dynamics*, *14*(1), 9–19.

Okano, K., Yamamoto, J., Okabayashi, T., Sugawara, Y., Shimada, K., Kosuge, T., et al. (2002). CT imaging of intrabiliary growth of colorectal liver metastases: A comparison of pathological findings of resected specimens. *The British Journal of Radiology*, *75*(894), 497–501.

Petri-Fink, A., Chastellain, M., Juillerat-Jeanneret, L., Ferrari, A., & Hofmann, H. (2005). Development of functionalized superparamagnetic iron oxide nanoparticles for interaction with human cancer cells. *Biomaterials*, *26*(15), 2685–2694.

Rappeport, E. D., & Loft, A. (2007). Liver metastases from colorectal cancer: Imaging with superparamagnetic iron oxide (SPIO)-enhanced MR imaging, computed tomography and positron emission tomography. *Abdom Imaging*, *32*(5), 624–634.

Ross, G. D., Vetvicka, V., Yan, J., Xia, Y., & Vetvickova, J. (1999). Therapeutic intervention with complement and beta-glucan in cancer. *Immunopharmacology*, *42*(1–3), 61–74.

Rummeny, E. J., & Marchal, G. (1997). Liver imaging: Clinical applications and future perspectives. *Acta Radiologica*, *38*(4 Pt 2), 626–630.

Suda, M., Ohno, N., Hashimoto, T., Koizumi, K., Adachi, Y., & Yadomae, T. (1996). Kupffer cells play important roles in the metabolic degradation of a soluble anti-tumor (1→3)-beta-D-glucan, SSG, in mice. *Fems Immunology and Medical Microbiology*, *15*(2–3), 93–100.

Suzuki, T., Ohno, N., Saito, K., & Yadomae, T. (1992). Activation of the complement system by (1→3)-beta-D-glucans having different degrees of branching and different ultrastructures. *Journal of Pharmacobio-dynamics*, *15*(6), 277–285.

Sveinbjornsson, B., Rushfeldt, C., Seljelid, R., & Smedsrod, B. (1998). Inhibition of establishment and growth of mouse liver metastases after treatment with interferon gamma and beta-1,3-D-glucan. *Hepatology*, *27*(5), 1241–1248.

Thornton, B. P., Vetvicka, V., Pitman, M., Goldman, R. C., & Ross, G. D. (1996). Analysis of the sugar specificity and molecular location of the beta-glucan-binding lectin site of complement receptor type 3 (CD11b/CD18). *Journal of Immunology*, *156*(3), 1235–1246.

Vu-Quang, H., Yoo, M.-K., Jeong, H.-J., Lee, H.-J., Muthiah, M., Rhee, J H., Lee, J.-H., Cho, C.S., Jeong, Y.Y. & Park, I.-K. Targeted delivery of mannan-coated superparamagnetic iron oxide nanoparticles to antigen presenting cells for magnetic resonance (MR)-based diagnosis of metastatic lymph node *in vivo*. Acta Biomaterialia, doi:10.1016/j.actbio.2011.06.044, in press.

Yoo, M. K., Park, I. Y., Kim, I. Y., Park, I. K., Kwon, J. S., Jeong, H. J., et al. (2008). Superparamagnetic iron oxide nanoparticles coated with mannan for macrophage targeting. *Journal of Nanoscience and Nanotechnology*, *8*(10), 5196–5202.